

Обзор ArXiv: astro-ph, 9-21 декабря 2023

От Сильченко О.К.

ArXiv: 2312.07070

The thickness of galaxy disks from $z=5$ to 0 probed by JWST

JIANHUI LIAN¹ AND LI LUO²

¹*South-Western Institute for Astronomy Research, Yunnan University, Kunming, Yunnan 650091, People's Republic of China*

²*School of Physics and Astronomy, China West Normal University, Nanchong, Sichuan 637009, People's Republic of China*

ABSTRACT

Although thick disk is a structure prevalent in local disk galaxies and also present in our home Galaxy, its formation and evolution is still unclear. Whether the thick disk is born thick and/or gradually heated to be thick after formation is under debate. To disentangle these two scenarios, one effective approach is to inspect the thickness of young disk galaxies in the high redshift Universe. In this work we study the vertical structure of 191 edge-on galaxies spanning redshift from 0.2 to 5 using JWST NIRCAM imaging observations. For each galaxy, we retrieve the vertical surface brightness profile at $1 R_e$ and fit a sech^2 function that has been convolved with the line spread function. The obtained scale height of galaxies at $z > 1.5$ show no clear dependence on redshift, with a median value in remarkable agreement with that of the Milky Way's thick disk. This suggests that local thick disks are already thick when they were formed in the early times and secular heating is unlikely the main driver of thick disk formation. For galaxies at $z < 1.5$, however, the disk scale height decreases systematically towards lower redshift, with low-redshift galaxies having comparable scale height with that of the Milky Way's thin disk. This cosmic evolution of disk thickness favors an upside-down formation scenario of galaxy disks.

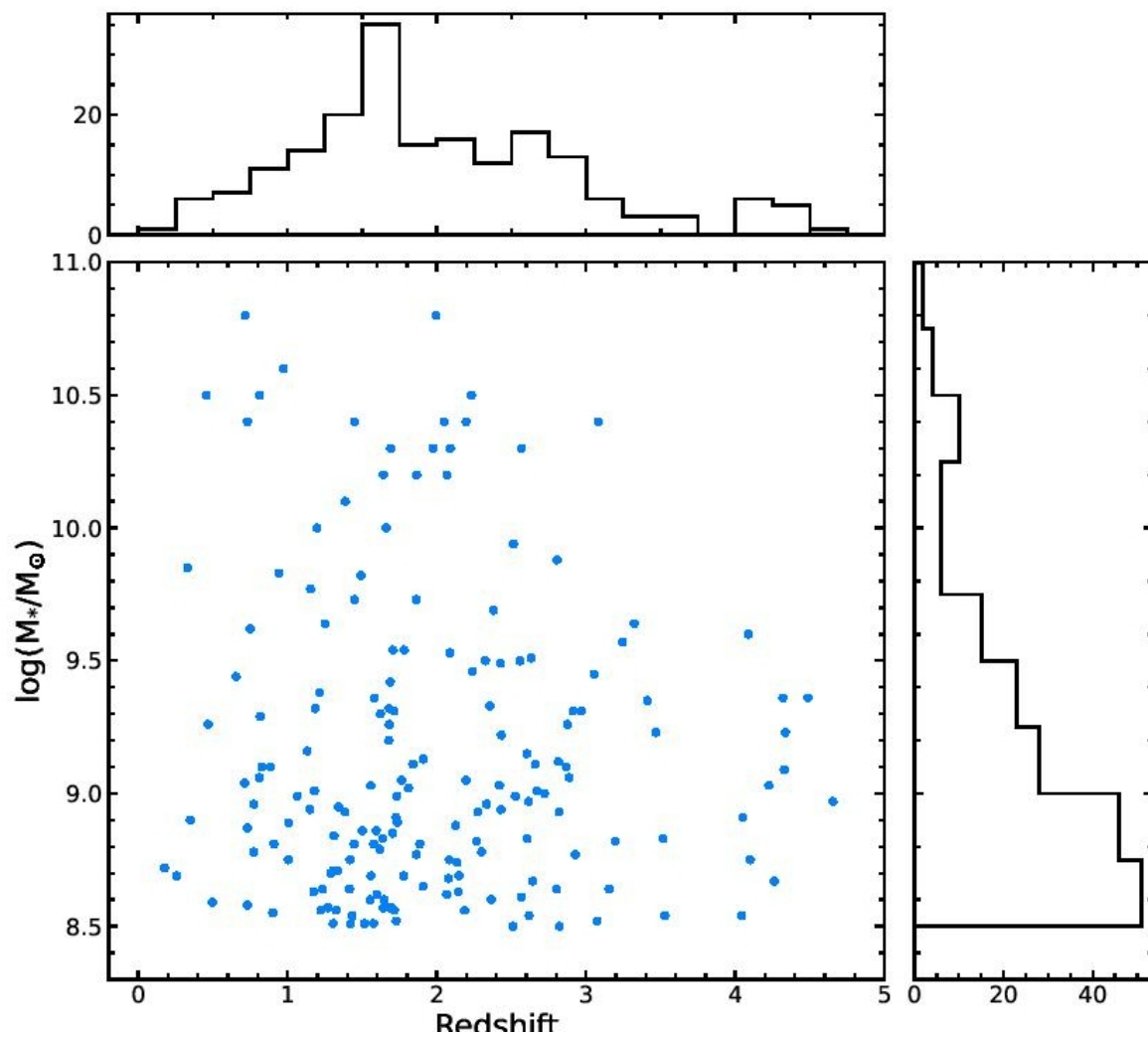
We focus on the JWST observations at one single band, F115W, which among all JWST filters has currently the longest exposure time in the CEERS survey and is a filter at short wavelength with relatively sharp PSF. In the released F115W images in the CEERS survey, a total number of 98149 sources are detected. For each source, we retrieve a 50×50 pixel ($\sim 2'' \times 2''$) image cut and obtain basic shape and photometry parameters (e.g., minor-to-major axis ratio, position angle) using SEXTRACTOR. We then measure the effective radii of these galaxies by extracting light profile using a series of ellipses with the same shape parameters derived above. Since the JWST CEERS field overlaps with the HST EGS field, we adopt the physical properties of these galaxies, including photometric/spectroscopic redshifts, stellar mass, and star formation rate (SFR) from public EGS catalogs (i.e., mass and redshift from [Stefanon et al. \(2017\)](#) and SFR from [Barro et al. \(2019\)](#)).

We then apply the following criteria to select our sample of edge-on galaxies:

- edge-on with axes ratio < 0.4 ;
- relatively massive with stellar mass $\log(M_*/M_\odot) > 8.5$;
- star forming with specific star formation rate $\log(\text{sSFR}/\text{yr}^{-1}) > -11$;
- redshift between 0 and 5.

A number of 352 galaxies satisfy these criteria. By visual inspection, we further remove 161 galaxies which are either wings of bright stars, part of nearby spiral galaxies, or close to companion galaxies or bright stars. Finally, the remaining 191 galaxies consist of our edge-on galaxy sample. For three of them, spectroscopic redshift is available.

Выборка



В разрез поперек диска (на эффективном радиусе) вписывают:

To measure the disk thickness of our edge-on galaxies, we first retrieve the vertical surface brightness profile (VSBP) at $1 R_e$, which is represented by the median profile between 0.5 and $1.5 R_e$. The vertical density profiles of galactic disks are well described by sech^2 function (e.g., Xiang et al. 2018; Hamilton-Campos et al. 2023). We therefore fit the VSBP of our galaxies with a sech^2 function

$$\Sigma = \mu_0 \times \frac{4}{(e^{\Delta z/h_z} + e^{-\Delta z/h_z})^2}$$

that has been convolved with the LSF obtained in §2.2. Here μ_0 and h_z are the central surface brightness and the scale height, respectively. The sech^2 function approximates exponential form at large distance, but the scale height in the sech^2 function is one-half of the exponential scale height.

Индивидуальные примеры

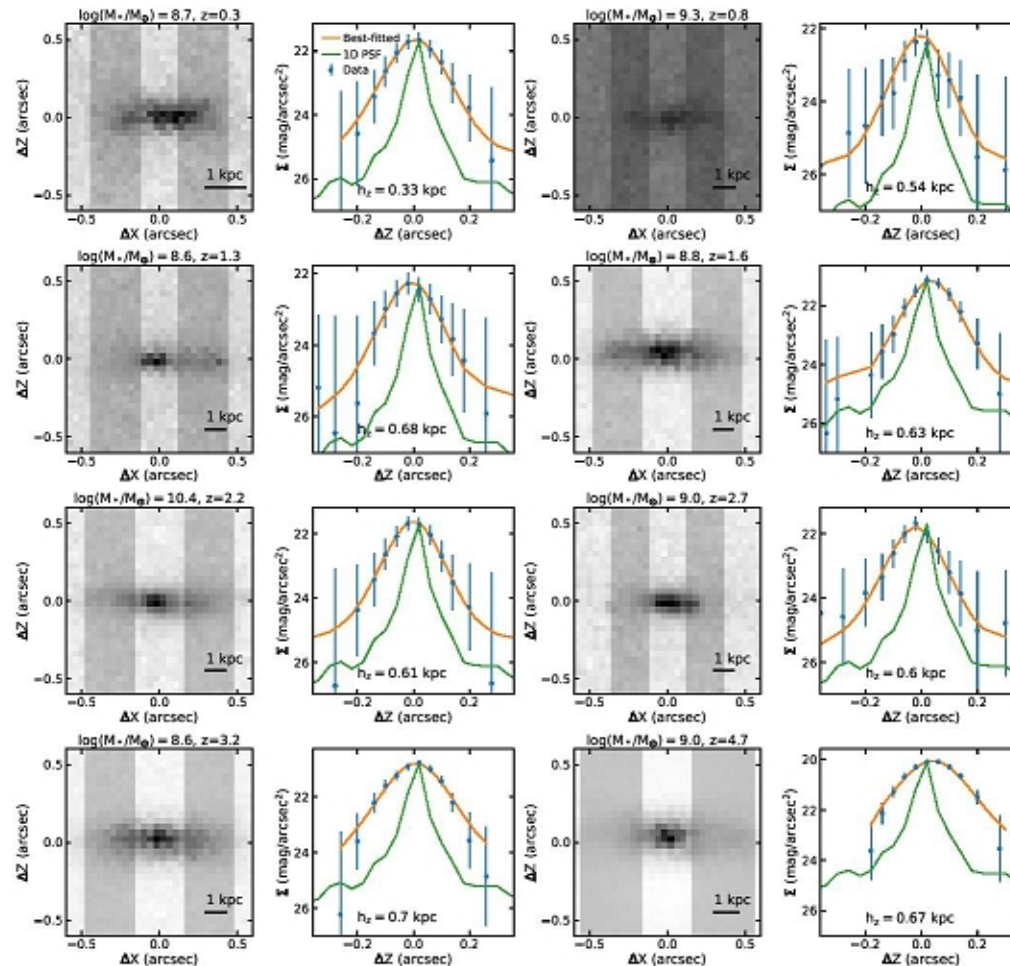
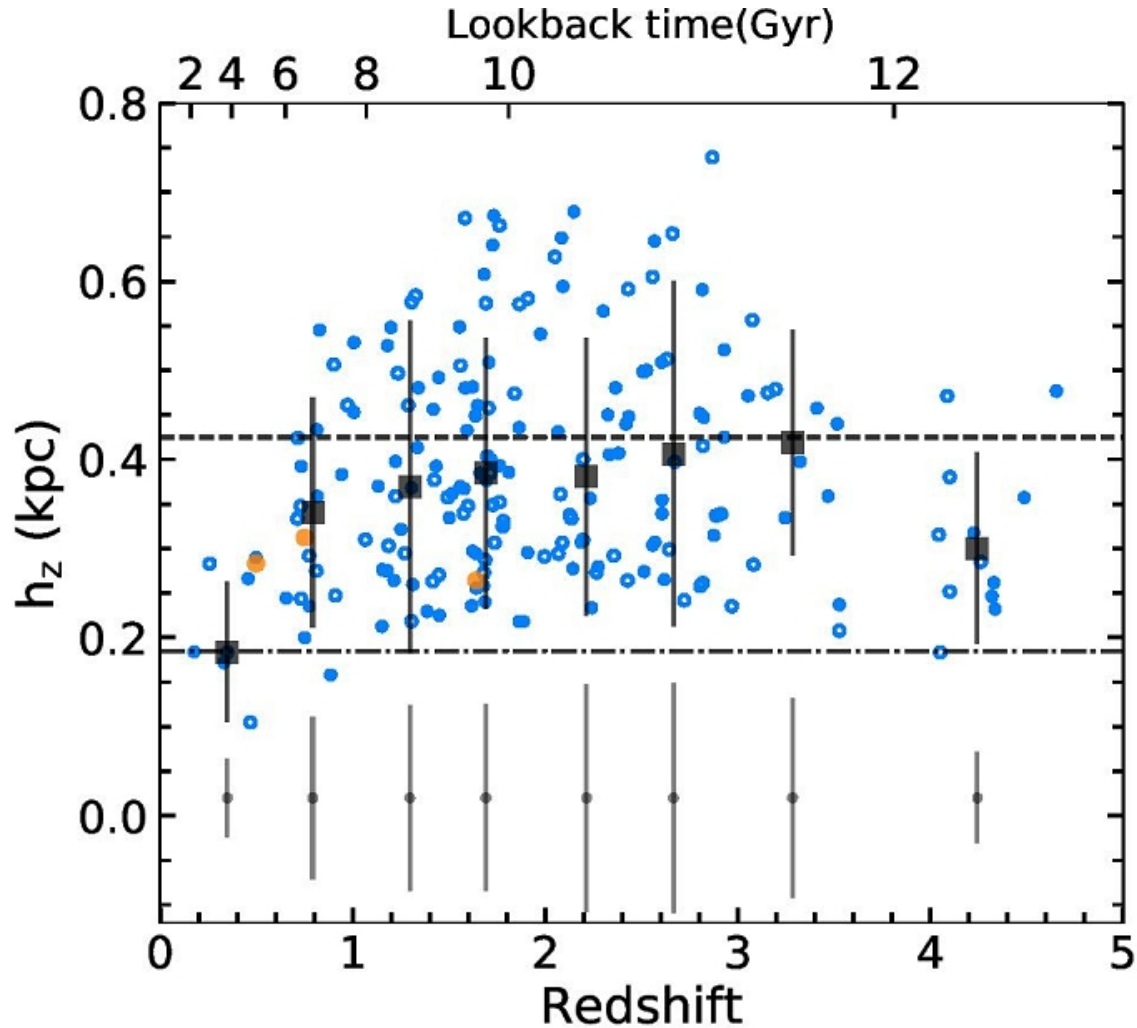


Figure 3. JWST/F115W images and vertical surface brightness profiles of eight example galaxies from low redshift at top left to high redshift at bottom right. In the image, the two gray shaded regions cover the pixels within 0.5 – $1.5 R_e$. The length of 1 kpc at each corresponding redshift is illustrated at the bottom right corner of the image. In the VSBP panel, the retrieved VSBP and best-fitted sech^2 model are shown as blue points and orange curve. The obtained sech^2 scale length is presented at the bottom. The line spread function obtained in §2.2 is also included as reference.

Главный результат



В бинах по красному смещению

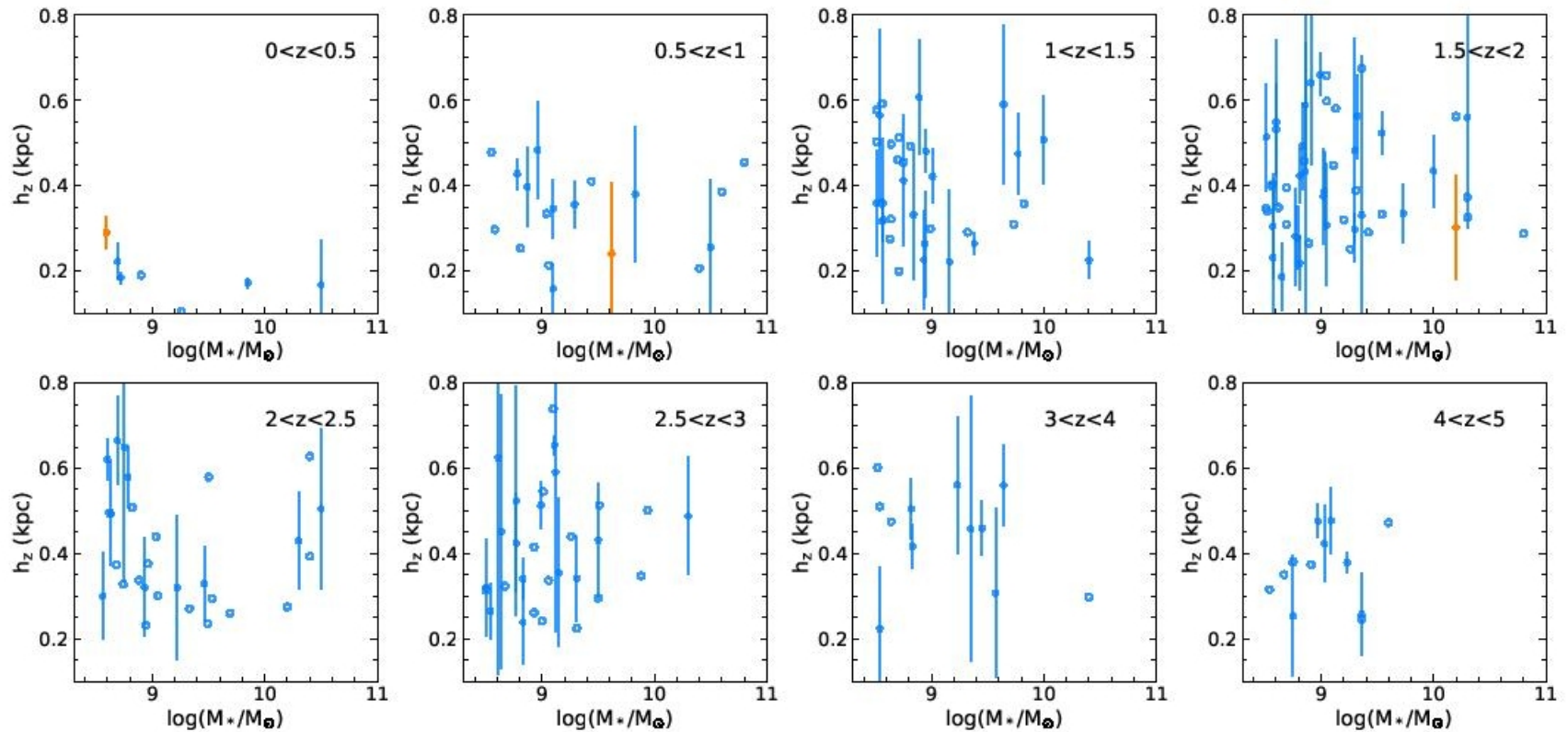






Figure 5. Scale height as a function of stellar mass for galaxies in eight redshift bins. Each panel shows edge-on galaxies in one redshift bin. The symbols are the same as Figure 4.

ArXiv: 2312.06880

Detection of diffuse H I emission in the circumgalactic medium of NGC 891 and NGC 4565 - II

Sanskriti Das ^{1,2}★ Mary Rickel ² Adam Leroy,^{2,3} Nickolas M. Pingel ^{4,5} D. J. Pisano,⁶
George Heald,⁷ Smita Mathur ^{2,3} Joshua Kingsbury,² and Amy Sardone²

¹*Kavli Institute for Particle Astrophysics & Cosmology, Stanford University, 452 Lomita Mall, Stanford, CA 94305, USA*

²*Department of Astronomy, The Ohio State University, 140 West 18th Avenue, Columbus, OH 43210, USA*

³*Center for Cosmology and Astroparticle Physics, 191 West Woodruff Avenue, Columbus, OH 43210, USA*

⁴*Research School of Astronomy & Astrophysics, Australian National University, Canberra, ACT 2611, Australia*

⁵*Department of Astronomy, The University of Wisconsin–Madison, 475 N. Charter Street, Madison, WI 53706, USA*

⁶*Department of Astronomy, University of Cape Town, Rondebosch 7700, Western Cape, South Africa*

⁷*CSIRO Astronomy and Space Science, PO Box 1130, Bentley, WA 6102, Australia*

13 December 2023

ABSTRACT

We probe the neutral circumgalactic medium (CGM) along the major axes of NGC 891 and NGC 4565 in 21-cm emission out to $\gtrsim 100$ kpc using the Green Bank Telescope (GBT), extending our previous minor axes observations. We achieve an unprecedented 5σ sensitivity of $6.1 \times 10^{16} \text{ cm}^{-2}$ per 20 km s^{-1} velocity channel. We detect H I with diverse spectral shapes, velocity widths, and column densities. We compare our detections to the interferometric maps from the Westerbork Synthesis Radio Telescope (WSRT) obtained as part of the HALOGAS survey. At small impact parameters, $> 31 - 43\%$ of the emission detected by the GBT cannot be explained by emission seen in the WSRT maps, and it increases to $> 64 - 73\%$ at large impact parameters. This implies the presence of diffuse circumgalactic H I. The mass ratio between H I in the CGM and H I in the disk is an order of magnitude larger than previous estimates based on shallow GBT mapping. The diffuse H I along the major axes pointings is corotating with the H I disk. The velocity along the minor axes pointings is consistent with an inflow and/or fountain in NGC 891 and an inflow/outflow in NGC 4565. Including the circumgalactic H I, the depletion time and the accretion rate of NGC 4565 are sufficient to sustain its star formation. In NGC 891, most of the required accreting material is still missing.

Green-Bank: NGC 891

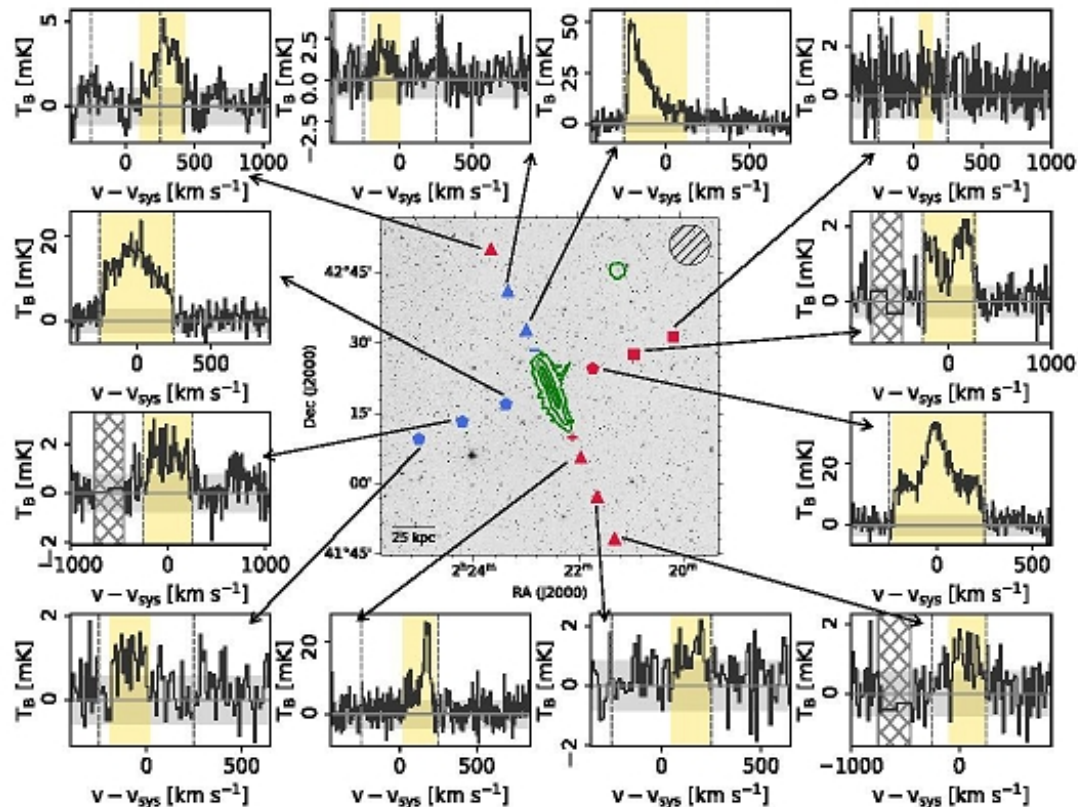


Figure 1a. The 21-cm emission spectra for the observed GBT pointings in the CGM of NGC 891, smoothed and re-binned at δv (see Table 1). The green contours on the Digitized Sky Survey (DSS) image show the integrated 21-cm intensity from the HALOGAS survey, with the lowest contour showing an H I column density of 10^{19} cm^{-2} . The GBT pointings observed in 15B-257, 20B-360, and 21B-324 are illustrated with pentagons, triangles, and squares on the DSS image, with red/blue symbols implying the mean line-of-sight velocity of the detected emission being positive/negative (arrows directed from pointings toward respective spectra). The direction of disk rotation has also been marked with '+/-' symbols at the edges of the H I disk. The GBT beam (hatched circle) and the scale are shown at the top and the bottom of the DSS image, respectively. The companion galaxy UGC 1807 is visible to the northwest of NGC 891. In each panel of the spectrum, the maximum rotational velocity of the H I disk is marked with vertical dashed gray lines, with the systemic velocity of NGC 891, 528 km s^{-1} , subtracted from the actual line-of-sight velocity. The horizontal gray patch denotes the $\pm \text{RMS}$ value of T_{B} . The horizontal gray line has been drawn at $T_{\text{B}} = 0$ to guide the eye. The vertical hatched region shown in some of the panels is the velocity region of the Milky Way that has been masked throughout the data reduction and analysis. We calculate the integrated intensity at each pointing by summing T_{B} over the velocity range shaded in yellow. At the pointings far from the disk, we detect emission signature at a level of $N(\text{H I}) = 1.3 - 13.2 \times 10^{17} \text{ cm}^{-2}$.

Green-Bank: NGC 4565

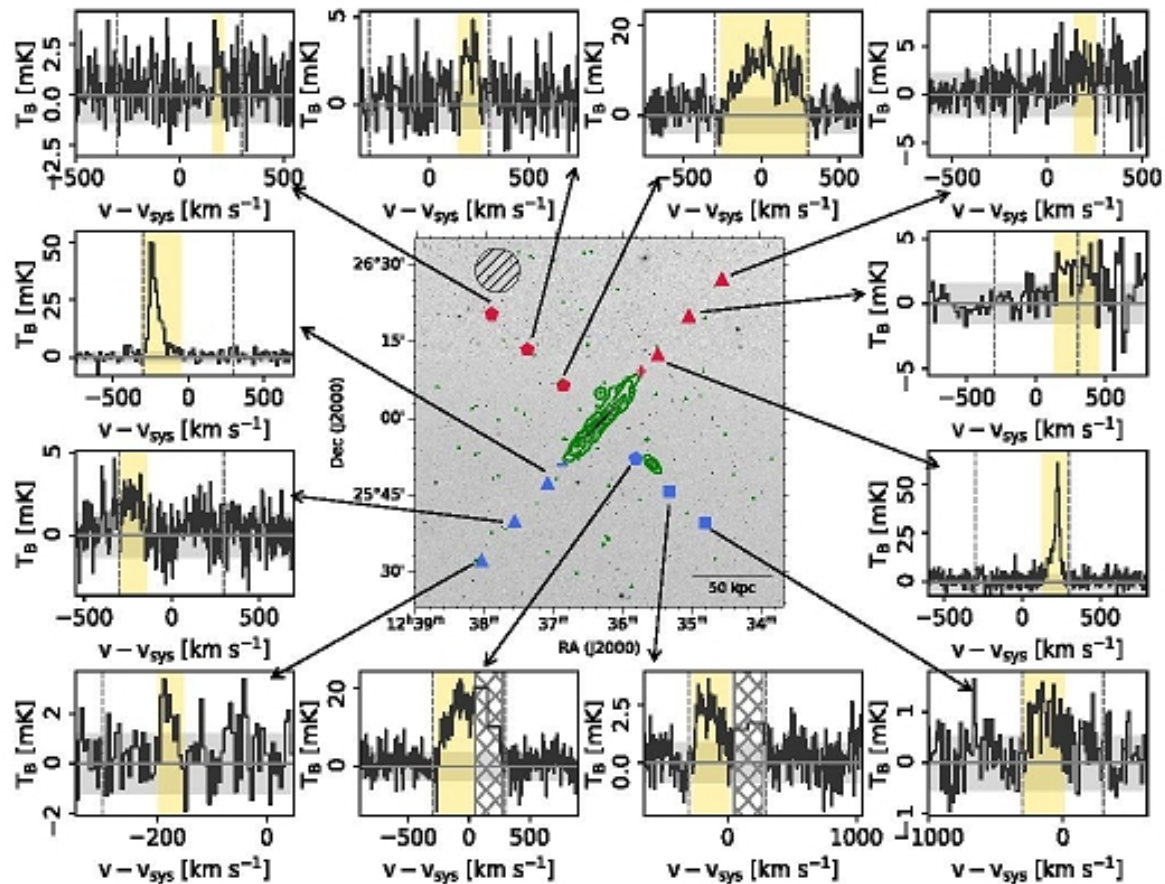


Figure 1b. The 21-cm emission spectra for the observed GBT pointings in the CGM of NGC 4565. The systemic velocity of NGC 4565, 1230 km s^{-1} , has been subtracted from the actual line-of-sight velocity in each spectrum. The companion galaxy NGC 4562 is visible to the southwest of NGC 4565. The vertical hatched region shown in some panels of the spectrum is the velocity region of NGC 4562 that has been masked throughout the data reduction and analysis. See the caption of Fig. 1a for more details.

Диффузного HI значительно больше, чем думали раньше

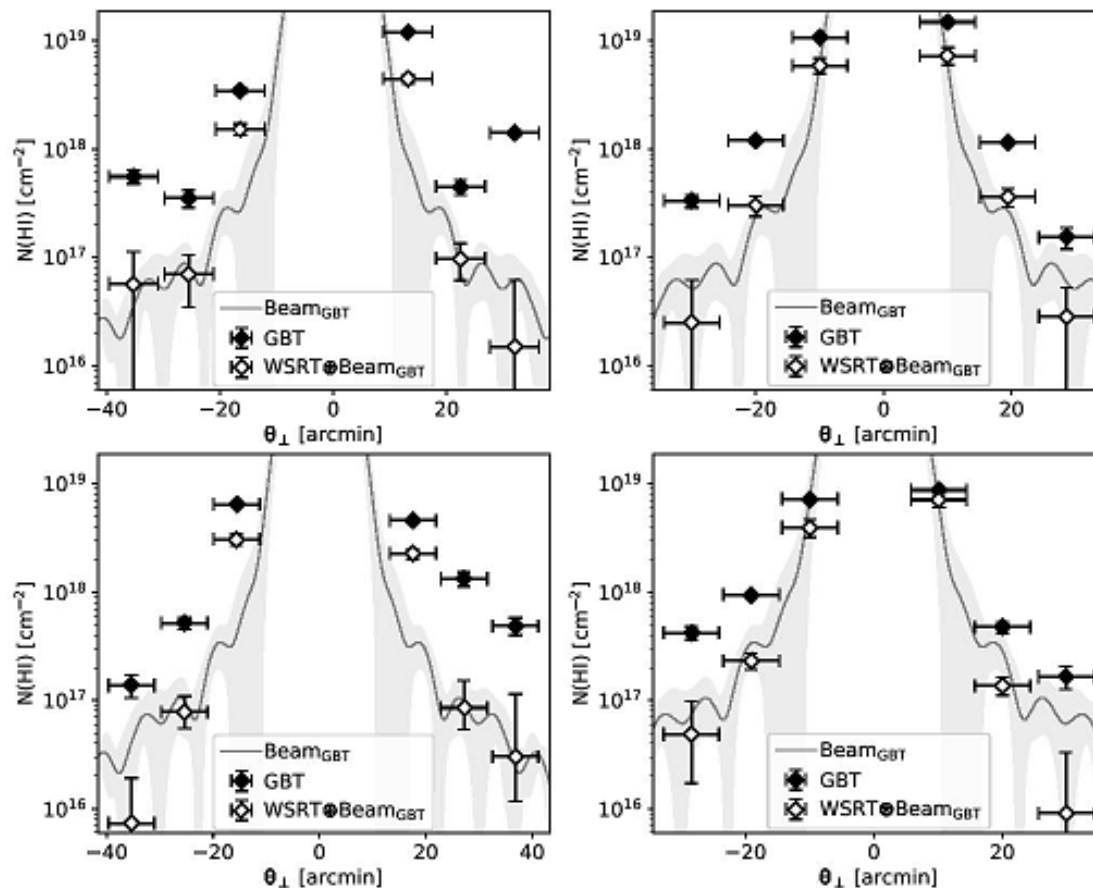


Figure 2. The radial $N(\text{HI})$ profile of NGC 891 (top) and NGC 4565 (bottom) along their major axes (left) and minor axes (right). The pointings at higher/lower declination than the galaxy disk are plotted at positive/negative angular separation from the galaxy center, respectively. The error bars along the y-axis include systematic uncertainties and statistical uncertainties. The error bars along the x-axis denote the GBT beam size. In our GBT data, systematic uncertainties come from the difference in T_{GB} across different sessions. In the WSRT data, systematic uncertainties come from the difference in masking threshold ($S/N > 4-5-6$), and circularization of the GBT beam. The shaded region around the beam model is 1σ uncertainty in the beam response due to averaging the beam map to one dimension. The positive offset between our GBT data and the convolved WSRT data indicates the presence of diffuse circumgalactic HI.

Профиль по малой оси – круче, чем по большой

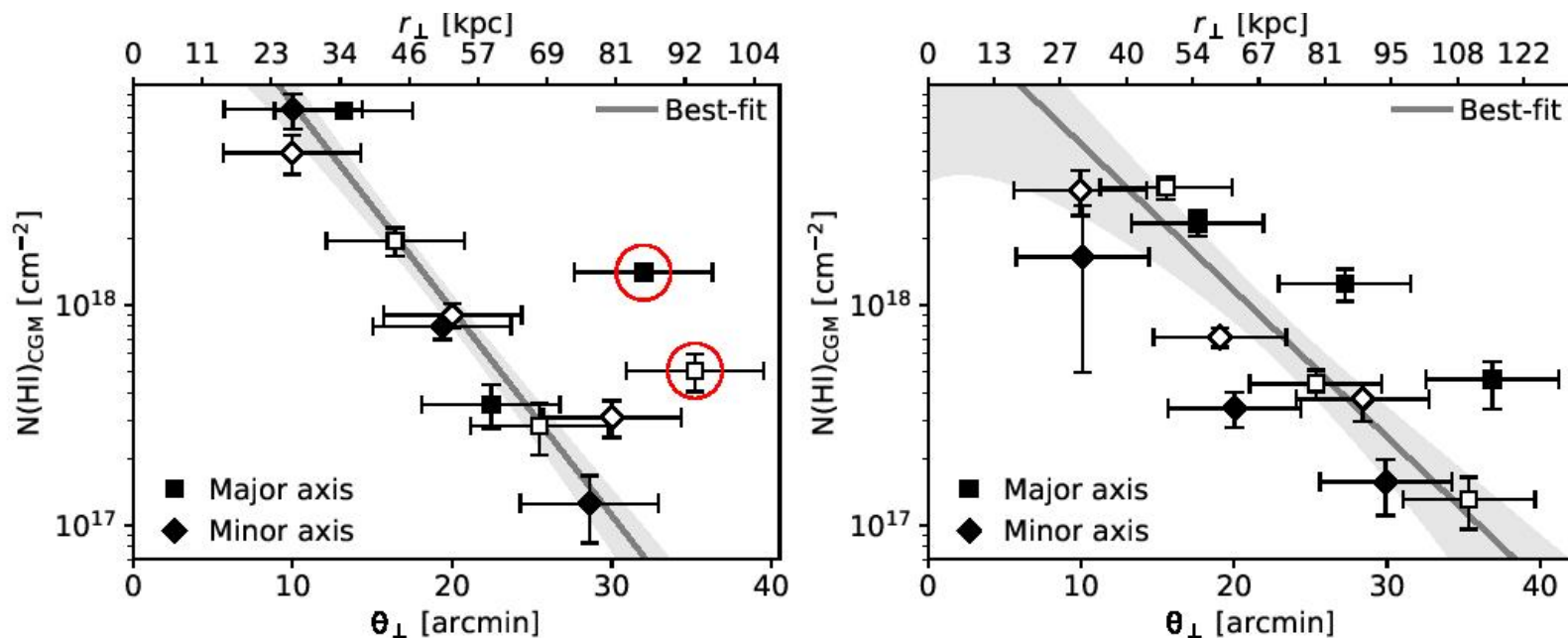


Figure 3. $N(\text{HI})$ in the CGM of NGC 891 (left) and NGC 4565 (right), with best-fit models. The filled and unfilled symbols correspond to pointings at higher and lower declinations than the galaxy disk. The physical separation corresponding to the angular separation from the disks is noted in the top x-axis, adopting a distance of 9.2 Mpc and 10.8 Mpc for NGC 891 and NGC 4565 from us, respectively (Heald et al. 2012). In the left panel, the points marked within red circles have been excluded from the fit. NGC 891 has a steeper profile than NGC 4565, with more H I closer to the disk of NGC 891.

Полная масса диффузного HI и темпы аккреции

For NGC 891 (excluding the UP3J/DN3J pointings), $M(\text{HI})_{\text{CGM}}$ along and around (within $\pm\pi/4$) the major and minor axes are $3.2 \pm 1.7 \times 10^8 M_{\odot}$ and $1.4 \pm 0.2 \times 10^8 M_{\odot}$, respectively, resulting in total mass of $4.6 \pm 1.7 \times 10^8 M_{\odot}$. For NGC 4565, $M(\text{HI})_{\text{CGM}}$ along and around the major and minor axes are $2.9 \pm 0.6 \times 10^8 M_{\odot}$ and $1.0 \pm 0.2 \times 10^8 M_{\odot}$, respectively, resulting in the total mass of $3.9 \pm 0.6 \times 10^8 M_{\odot}$.

Thus, both galaxies have more mass along the major axes than the minor axes, indicating active accretion along the major axes. The masses quoted in D20 based on minor axes pointings and assuming azimuthal symmetry were underestimated.

$M(\text{HI})_{\text{CGM}}$ is $11.4 \pm 4.2\%$ and $5.4 \pm 0.8\%$ of the $M(\text{HI})_{\text{disk}}$ of NGC 891 and NGC 4565, respectively. Based on the GBT and WSRT measurements within 50 kpc of NGC 891 and NGC 4565, P18 estimated f_{19} , the fraction of HI mass below $N(\text{HI}) = 10^{19} \text{ cm}^{-2}$ to be 0.4–0.6% and 0.7–0.9%, respectively. Our measurement is larger than the estimation of P18 by an order of magnitude. It suggests the presence of a large amount of diffuse, extended HI with $N(\text{HI})$ below 10^{19} cm^{-2} , extending beyond 50 kpc. This emission might have been missed due to the lower sensitivity of the GBT observations presented in P18. Also, f_{19} in P18 was based on azimuthal averages in circular annuli around the galaxies, whereas we focus on pointings along principal axes. Therefore, most of the circumgalactic HI could be concentrated along principal axes of the galaxies, leading to a higher estimate in our case.

The depletion timescale, $\tau_{\text{dep}} = (M(\text{HI})_{\text{disk}} + M(\text{HI})_{\text{CGM}})/\text{SFR}$ is $2.1 \pm 0.8 \text{ Gyr}$ for NGC 891 and $11.4 \pm 1.8 \text{ Gyr}$ for NGC 4565. By

4.4 Accretion rate

In NGC 891, the total accretion rate, \dot{M}_{CGM} , at the position of all observed pointings integrated within the GBT beam is $0.30 \pm 0.03 M_{\odot} \text{ yr}^{-1}$. For all pointings except UP3J and DN3J (as they were excluded from the fitting of $N(\text{HI})_{\text{CGM}}$ in §4.1), we extend the accretion rate calculation to each quadrant in the CGM (i.e., $\pm\pi/4$ region around the major and minor axes) assuming azimuthal symmetry, and obtain \dot{M}_{CGM} of $0.73 \pm 0.08 M_{\odot} \text{ yr}^{-1}$. Adding it to the accretion rate measured within the GBT beam of the excluded pointings, the total \dot{M}_{CGM} is $0.80 \pm 0.08 M_{\odot} \text{ yr}^{-1}$. \dot{M}_{CGM} along the major and minor axes are $0.65 \pm 0.08 M_{\odot} \text{ yr}^{-1}$ and $0.15 \pm 0.01 M_{\odot} \text{ yr}^{-1}$.

In NGC 4565, the total \dot{M}_{CGM} at the position of all observed pointings integrated within the GBT beam is $0.20 \pm 0.02 M_{\odot} \text{ yr}^{-1}$. Extending the accretion rate calculation to each quadrant in the halo, we obtain a total \dot{M}_{CGM} of $0.83 \pm 0.08 M_{\odot} \text{ yr}^{-1}$. \dot{M}_{CGM} along the major and minor axes are $0.66 \pm 0.07 M_{\odot} \text{ yr}^{-1}$ and $0.17 \pm 0.03 M_{\odot} \text{ yr}^{-1}$.

Using the second definition of accretion rate (equation 5b), \dot{M}_{CGM} along the major axes of NGC 891 and NGC 4565 are $0.29 \pm 0.04 M_{\odot} \text{ yr}^{-1}$ and $0.57 \pm 0.06 M_{\odot} \text{ yr}^{-1}$, respectively.

Спин диффузного газа – соответствует дискам галактик

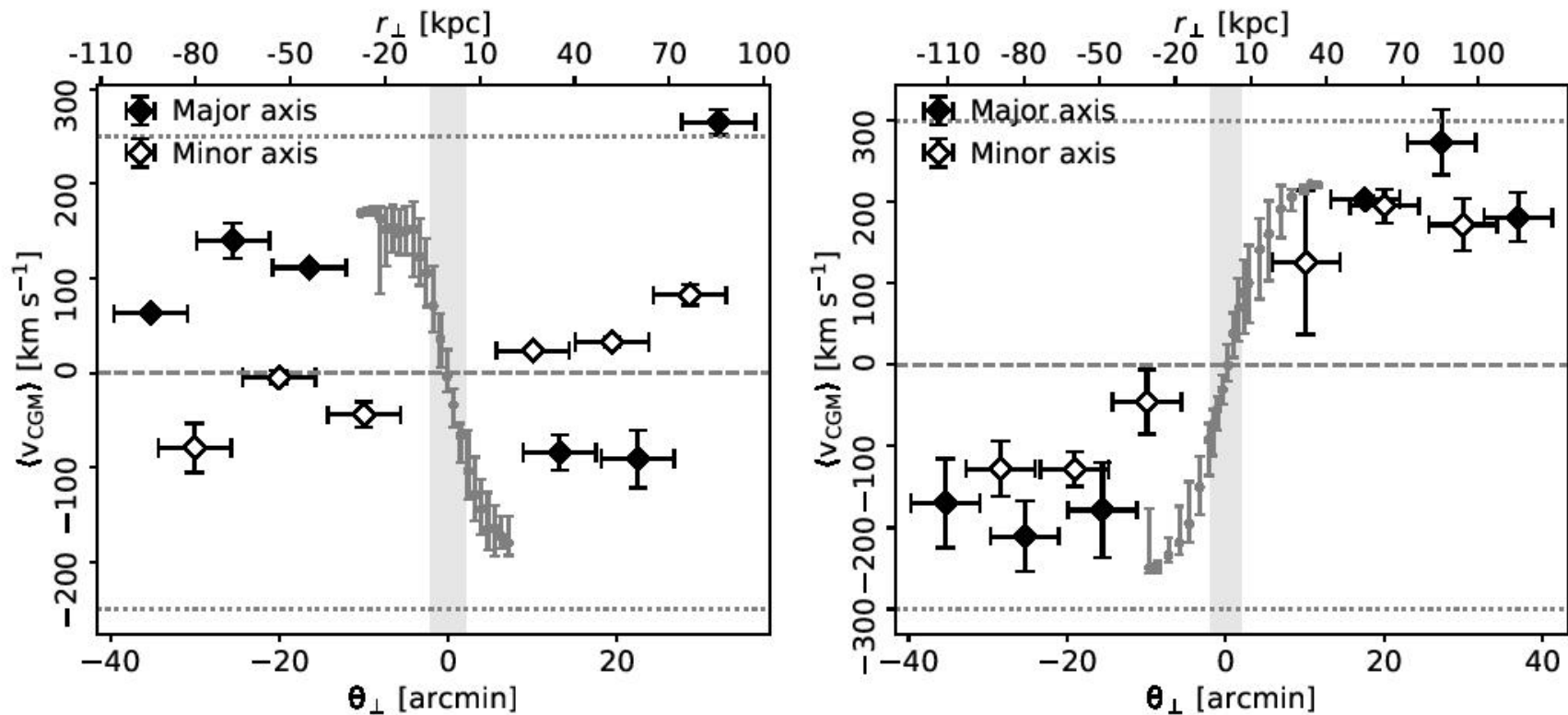


Figure 5. The line-of-sight mean velocity of H I in the CGM of NGC 891 (left) and NGC 4565 (right) in the rest frame of the galaxy. The horizontal dotted lines denote the maximum rotational velocity of the H I disk measured in the GBT data. The gray circles show the rotation curve of the disk along the major axis, measured in the WSRT data. The spatial extent of the disk along the minor axis is shown with the gray vertical patch. The horizontal dashed line is drawn at 0 km s⁻¹ to guide the eye.

ArXiv: 2312.09567

Discovery of a large-scale H I plume in the NGC 7194 Group

MINA PAK,^{1,2} JUNHYUN BAEK,³ JOON HYEOP LEE,⁴ AEREE CHUNG,³ MATT OWERS,^{1,2} HYUNJIN JEONG,⁴
EON-CHANG SUNG,⁴ AND YUN-KYEONG SHEEN⁴

¹*School of Mathematical and Physical Sciences, Macquarie University, NSW 2109, Australia*

²*ARC Centre of Excellence for All Sky Astropysics in 3 Dimensions (ASTRO 3D), Australia*

³*Department of Astronomy, Yonsei University, 50 Yonsei-ro, Seodaemun-gu, Seoul, 03722, Republic of Korea*

⁴*Korea Astronomy and Space Science Institute (KASI), 776 Daeduk-daero, Yuseong-gu, Daejeon 34055, Republic of Korea*

ABSTRACT

We present the discovery of a new H I structure in the NGC 7194 group from the observations using the Karl G. Jansky Very Large Array. NGC 7194 group is a nearby ($z \sim 0.027$) small galaxy group with five quiescent members. The observations reveal a 200 kpc-long H I plume that spans the entire group with a total mass of $M_{HI} = 3.4 \times 10^{10} M_{\odot}$. The line-of-sight velocity of the H I gas gradually increases from south (7200 km s^{-1}) to north (8200 km s^{-1}), and the local velocity dispersion is up to 70 km s^{-1} . The structure is not spatially coincident with any member galaxies but it shows close associations with a number of blue star-forming knots. Intragroup H I gas is not rare, but this particular structure is still one of the unusual cases in the sense that it does not show any clear connection with sizable galaxies in the group. We discuss the potential origins of this large-scale H I gas in the NGC 7194 group and its relation with the intergalactic star-forming knots. We propose that this HI feature could have originated from tidal interactions among group members or the infall of a late-type galaxy into the group. Alternatively, it might be leftover gas from flyby intruders.

Группа NGC 7194



Глубокие наблюдения в 21 см

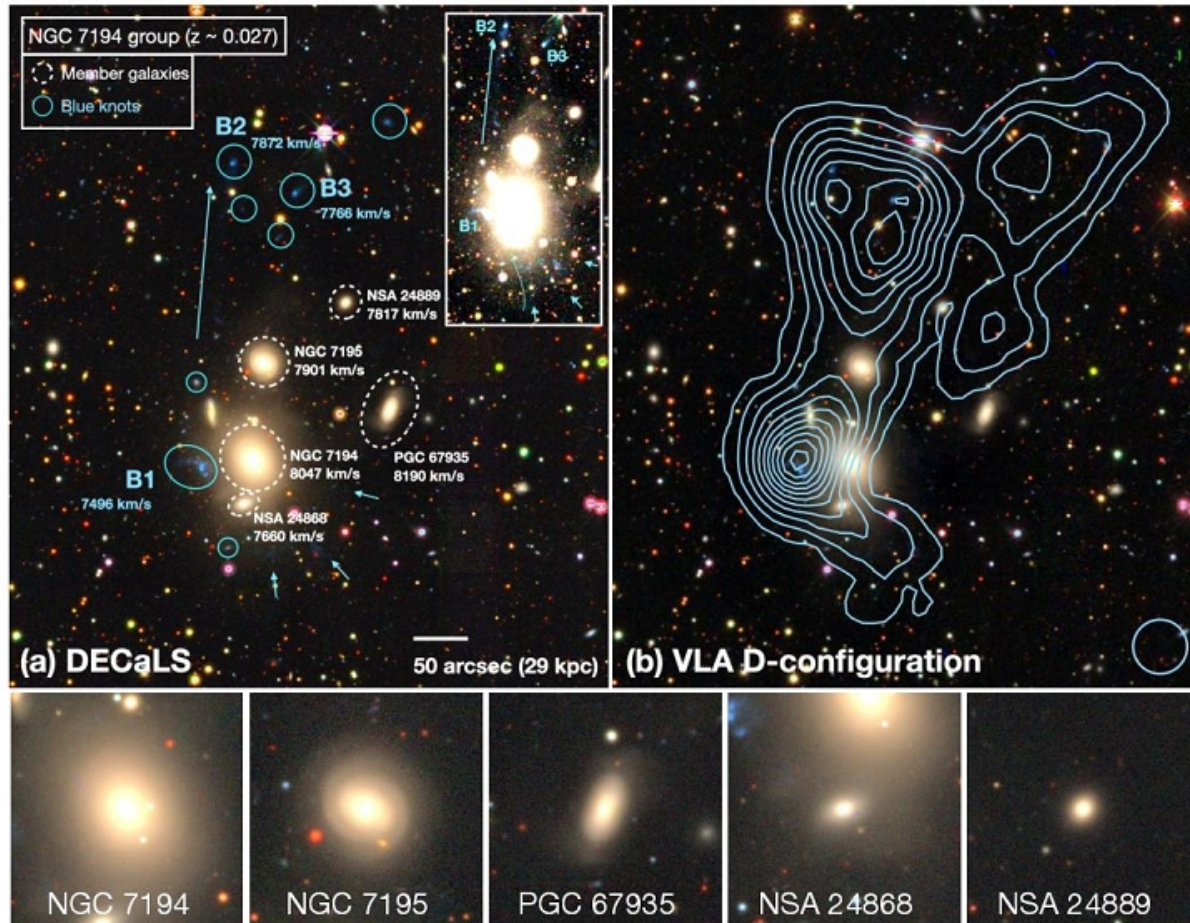


Figure 1. (a) The DECaLS image of the NGC 7194 group. North is at the top and east is to the left. White dotted circles are the five previously-known members of the group. Cyan circles are blue knots. The long arrow is drawn parallel with the long diffuse and blue stream, and the small arrows mark diffuse blue branches in the south-western outskirts of the N7194. (b) H I distributions from VLA D-configuration is overlaid on the DECaLS image. Circle in the right-bottom corner denotes the beam size of D-configuration. The contour levels of H I column density go from 1.5 to $47.0 \times 10^{19} \text{ cm}^{-2}$ in the interval with 10 steps in linear scale. The DECaLS images ($70'' \times 70''$) of five quiescent galaxies are shown in the bottom panel. The IDs of NSA 24868 and NSA 24889 are taken from the NASA-Sloan Atlas catalog (NSA, Blanton et al. 2011).

Облако вращается? Или это «неплоское» падение?

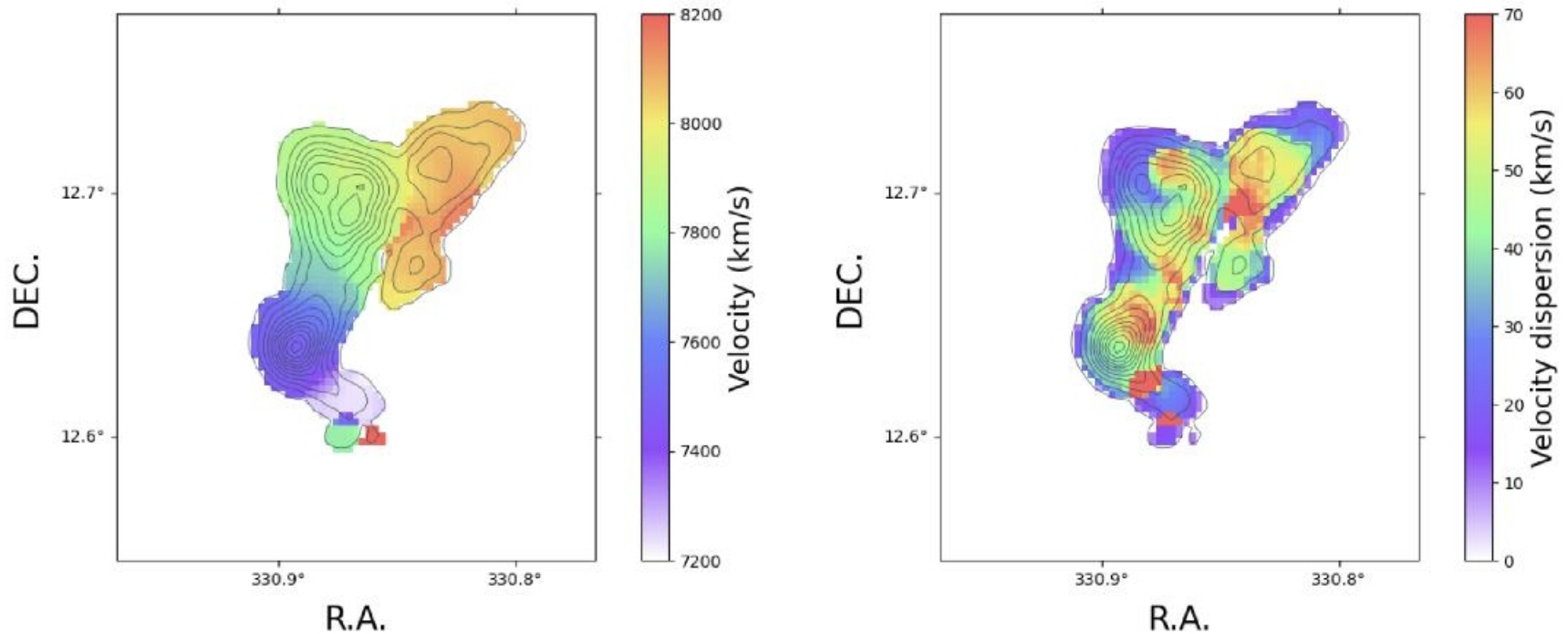
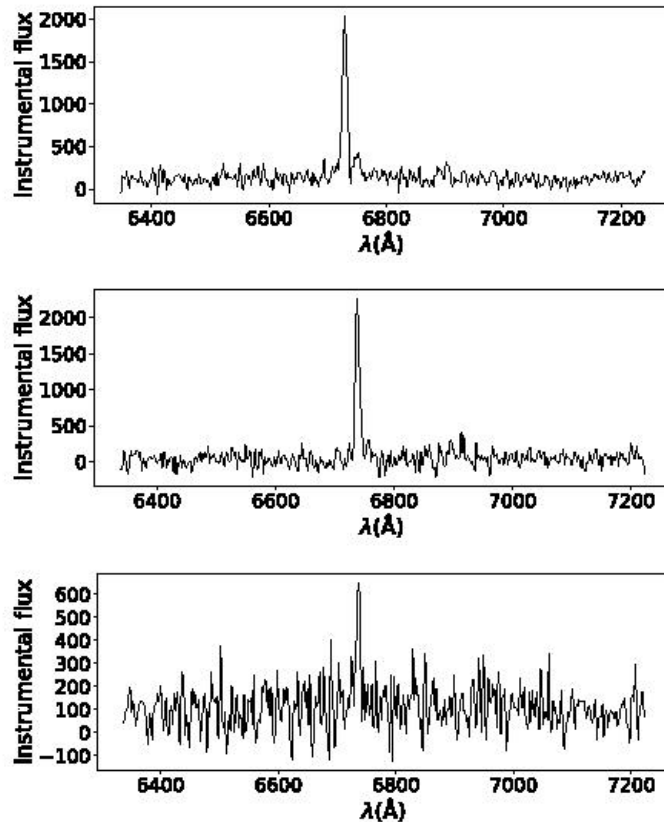


Figure 2. The H I intensity weighted velocity (left panel) and velocity dispersion (right panel) from VLA D-configuration. H I column density contours are overlaid with solid lines on both maps. The H I velocities increase smoothly from 7200 km s^{-1} in the south to 8200 km s^{-1} in the north.

До кучи – досняли эмиссионные спектры для голубых сгустков



Это H α -области!

Figure 3. The spectra of three blue knots (B1 - B3) observed from the Doyak 1.8-m telescope of Bohyunsan Optical Astronomy Observatory long-slit spectrograph. We detected H α emission centered at 7496, 7872, and 7766 km s^{-1} , respectively. Instrumental flux is shown since calibration is not applied since signal to noise of the continuum is not sufficient enough to analyze flux calibration.

Три сценария:

- Ободрать NGC 7195?
- Разодрать бывшую спираль, от которой осталось только В1?
- Пропустить через группу большую галактику, отняв у нее газ? Но кандидат – PGC 67927 – до сих пор БОГАТ газом

Ни один не работает!